Chinese Journal of Polymer Science Vol. 34, No. 4, (2016), 407–419

Chinese Journal of Polymer Science

Decyloxyphenyl-substituted Quinoxaline-embedded Conjugated Electrochromic Polymers with High Switching Stability and Fast Response Speed*

Zhen Xu[a], Ling-qian Kong[b], Jin-sheng Zhao[c**] and Wei-yu Fan[a**]

[a] *State Key Laboratory of Heavy Oil Processing, China University of Petroleum (East China), Qingdao 266555, China*
[b] *Dongchang College, Liaocheng University, Liaocheng 252059, China*
[c] *Shandong Key Laboratory of Chemical Energy Storage and Novel Cell Technology, Liaocheng University, Liaocheng 252059, China*

Abstract Two novel decyloxyphenylquinoxaline-based donor-acceptor (D-A) electroactive monomers bearing dialkoxythiophene as the donor unit are synthesized using Stille coupling reaction. The corresponding polymers, poly[2,3-bis(4-decyloxyphenyl)-5,8-bis(3,4-dimethoxylthiophen-2-yl)quinoxaline] (**P1**) and poly[2,3-bis(4-decyloxyphenyl)-5,8-bis(2,3-dihydrothieno[3,4-b][1,4]dioxin-5-yl)quinoxaline] (**P2**), are directly deposited onto the working electrode surface by electropolymerization. All materials were characterized by nuclear magnetic resonance (NMR), mass spectrometry (MS), scanning electron microscopy (SEM), cyclic voltammetry (CV), ultraviolet-visible absorption spectrometry (UV-Vis) and spectro-electrochemical measurements. Electrochemical studies demonstrate that both polymers are capable of showing both reasonable n- and p-doping processes, and advanced long-term switching stabilities. 3,4-Ethylenedioxythiophene substituted for 3,4-dimethoxythiophene as a donor unit, which enhances the conjugated double-bond character of the conducting polymer, thus leading to a lower electronic band-gap. Likewise, the neutral state color of the synthesized polymer tuned from blue to blue-green corresponding to the red shift of the maximum absorption wavelengths in the visible region. In addition, kinetics study of **P1** revealed 42% (595 nm), 30% (839 nm) and 69% (1500 nm) transmittance changes (ΔT%), while **P2** exhibited 32% (740 nm), 71% (2000 nm) at the dominant wavelengths. It was also observed that both films could switch quickly between the neutral state and oxidation state, with the response time less than 1 s both in visible and near infrared regions.

Keywords: 3,4-Dimethoxythiophene; Decyloxyphenylquinoxaline; High switching stability; Fast response time.

Electronic Supplementary Material Supplementary material is available in the online version of this article at http://dx.doi.org/10.1007/s10118-016-1759-7.

INTRODUCTION

Conjugated organic conducting polymers (CPs), since their discovery, have drawn great attention as optoelectronic materials. Conjugated polymers allow their use in numerous application fields such as light-emitting diodes[1], field effect transistors[2], sensor devices[3, 4], electrochromic devices (ECDs)[5, 6], organic

* This work was financially supported by the National Natural Science Foundation of China (Nos. 51473074 and 31400044), the General and Special Program of the Postdoctoral Science Foundation China (Nos. 2013M530397 and 2014T70861), the Postgraduate Innovation Project of China University of Petroleum (East China) (No. YCX2015022) and the Fundamental Research Funds for the Central Universities (No. 15CX06049A).
** Corresponding authors: Jin-sheng Zhao (赵金生), E-mail: j.s.zhao@163.com
Wei-yu Fan (范维玉), E-mail: fanwyu@upc.edu.cn
Received October 1, 2015; Revised November 15, 2015; Accepted November 17, 2015
doi: 10.1007/s10118-016-1759-7

photovoltaics (OPVs)[7], solar cells[8] and supercapacitors[9]. A reversible color and transmissivity change in a material by altering their redox state is defined as electrochromism. The change of the spectral absorption bands upon doping and dedoping (valence electrons transition to different energy levels) resulted in the optical changes of the material. Band gap of electrochromic polymers is an extremely important parameter since it is directly related with the electron or hole affinities, absorption values and conductivities of polymers.

Recently, low band-gap polymers have caused more and more attention due to the numerous advantages, especially those polymers with band-gap value lower than 1.5 eV[10]. According to the donor-acceptor theory, the incorporation of the alternating electron donor and acceptor units on the backbone of polymer is the mostly used technique to design low band-gap polymers. This approach causes lower band-gap and wider band-width, which should be attributable to the increasing resonances that can strengthen double-bond character between the repeating units of a conjugated polymer[11]. The donor-acceptor systems are also expected to improve the stability of n-doping property which allows their usage in series of energy storage applications. Therefore, various low band-gap advanced conjugated polymers with superior optical and electrical properties have been synthesized following this approach.

Due to the strong conjugated π-bonds in the structures, benzothiadiazole[12], thieno[3,4-b]pyrazine[13] and 2,1,3-benzoselenadiazole[14] with the electron withdrawing imine (C＝N) have emerged as acceptor building blocks to synthesize organic electronics materials. However, significant advantages of quinoxaline acceptor can be found when compared to the aforementioned ones that quinoxaline (Qx) acceptors can be relatively easy to be functionalized with various aryl or alkyl groups, thus improving the optoelectronic properties of the corresponding conjugated polymers. So, in the recent work our group has focused on the synthesis and electro-optical characterization of low band-gap polymers incorporating various substituted quinoxalines (Qx) as acceptor[15–17]. As was expected, the materials possess green neutral state and transmissive oxidized state in addition to the stable n-doping process which can facilitate their use in smart window applications and light emitting displays. As for donor moiety, 3,4-ethylenedioxythiophene (EDOT) which is more electron-rich than thiophene is a great candidate to be used as donor units in the monomers obeying D-A theory. The presence of alkoxy substituent with strong electron-donor ability can enhance the resonance effects between the donor and acceptor units, thus leading to the formation of low band-gap polymers with low oxidation potential, easy switching between two redox states, and robust stabilities[18, 19].

In 2008, Gorkem *et al*. reported the first solution-processable poly(2,3-bis(3,4-bis(decyloxy)phenyl)-5,8-bis(2,3-dihydrothieno[3,4-b][1,4]dioxin-5-yl)quinoxaline) (PDOPEQ) film with a green neutral state and a highly transmissive oxidized state[20]. It has clearly been demonstrated that the introduction of alkyl side chains can not only enhance the ease of processing, but also modify the electronic properties of the conjugated polymers[21]. Long alkyl chains separate the polymer backbones from each other. Then, the distance between the backbones causes faster doping process and easy transfer of counter ions within the film which decreases the switching time. The oxidation potential[22], switching stability[23], and band-gap[24] of the polymers can be drastically altered by inserting strong electron-donating alkoxy side chains in the polymer backbone. Besides, alkyl chains can also increase the solubility of resulting polymers which is an important property in the application and processing[25].

Based on the previous work, we synthesized two new D-A type polymers that incorporate 3,4-dimethoxythiophene (**P1**) and 3,4-ethylenedioxythiophene (**P2**) as the donor units, and 2,3-bis(4-decyloxyphenyl)-quinoxaline containing only one decyloxy side chain as the acceptor unit. By comparison with PDOPEQ film[20], we found that the newly synthesized polymers had relatively good electrochemical cycle stability (loss of 10% after 5000 cycles for PDOPEQ, loss of 4% after 5000 cycles for **P2**), and significant fast discoloration response speed (less than 1 s for PDOPEQ, 0.3 s for **P2**), particularly those in near-infrared region. The presence of double-substituted long-chain alkyl group hindered the transfer of counter ions within the film and caused slower doping process which reduced the switching speed. In addition, the two new synthetic polymers exhibited stable electrochemical characteristics of n-type doping, while polymer PDOPEQ did not. Further, to gain deep insight into the geometric structures and electrical band gaps of the materials, quantum-

chemical simulations were performed and the results were compared with the corresponding experimental data. Additionally, the effects of different donor units on electrochemical and optical properties of the resulting polymers were also investigated.

EXPERIMENTAL

Materials and Instrumentation

Unless otherwise stated, all reagents and chemicals were purchased from Aldrich Chemical and used without further purification. 3,6-Dibromo-1,2-phenylenediamine (**2**)[26],1,2-bis(4-decyloxyphenyl) ethane-1,2-dione (**5**)[27] and tributylstannane compounds[28] were prepared according to the previously reported literature methods. The NMR spectra of the monomers were obtained on a Varian AMX 400 spectrometer in $CDCl_3$ at room temperature, and chemical shifts (δ) are given relative to tetramethylsilane as the internal standard, while the coupling constants (J) are given in Hz. Mass spectrometry analysis was conducted using a Brukerma Xis UHR-TOF mass spectrometer.

Electropolymerization and characterization of CV was performed with a CHI 760 C Electrochemical Analyzer in a three-electrode cell consisting of platinum wire with a diameter of 0.5 mm, platinum ring as the counter electrode, and Ag wire as the pseudo-reference electrode immersed in 0.2 $mol \cdot L^{-1}$ tetrabutylammonium hexafluorophosphate ($TBAPF_6$) as the supporting electrolyte.

Spectroelectrochemical and kinetic measurements were performed using absorption spectra of the polymer films upon applied potentials. The spectroelectrochemical cell includes a quartz cuvette, an Ag wire reference electrode (RE), a Pt wire counter electrode (CE), and ITO/glass as transparent working electrode (WE). The polymer films for spectroelectrochemistry were grown potentiostatically on ITO/glass electrode and the thickness was controlled by the total charge passed through the cell. Indium-tin-oxide-coated (ITO) glass (the active area: 0.9 cm × 2.0 cm; sheet resistance: < 10 $\Omega \cdot sq^{-1}$) should be cleaned successively by ethanol, acetone and deionized water under ultrasonic, and dried by N_2 flow before use.

Scanning electron microscopy (SEM) measurements were taken using a Hitachi SU-70 thermionic field emission scanning electron microscope with the polymer deposited on the indium-tin-oxide (ITO)-coated glass. The thickness and surface roughness of the polymer films were tested by a KLA-Tencor D-100 step profiler. UV-Vis-NIR spectra were recorded on a Varian Cary 5000 spectrophotometer with a measurement range extended from 200 nm to 3300 nm at a scan rate of 800 $nm \cdot min^{-1}$. Digital photographs of the polymer films were taken by a Canon Power Shot A3000 IS digital camera.

Synthesis

*3,6-Dibromo-1,2-phenylenediamine (**2**)*

To a suspension of 4,7-dibromo-2,1,3-benzothiadiazole (11.5 g) in EtOH (400 mL) was added excess amount of sodium borohydride ($NaBH_4$) (26.8 g) at 0 °C, and then the mixture was magnetically stirred for 36 h. Evaporation of the solvent followed by column chromatography from hexane: dichloromethane (3:1, *V*/*V*) gave 3,6-dibromo-1,2-phenylenediamine (**2**) (8.36 g) as a white solid in 84.7% yield. ^{1}H-NMR ($CDCl_3$, 400 MHz): δ = 6.83 (s, 2H), 3.87 (s, 4H) (See Supporting Information Fig. S1).

*1,2-Bis(4-decyloxyphenyl) ethane-1,2-dione (**5**)*

A mixture of 1,2-bis(4-methoxyphenyl) ethane-1,2-dione (3 g), glacial acetic acid (30 mL) and HBr (48%, 100 mL) boiled under a reflux condenser for 8 h, stirring constantly. After the mixture was cooled to room temperature, a brown solid was filtered, and washed with distilled water several times to give 1,2-bis(4-hydroxyphenyl) ethane-1,2-dione (**4**) in 78% yield. Next, to a solution of **4** (2.0 g) in 80 mL of *N*,*N*-dimethylformamide (DMF) was added 1-bromine decane (4.04 g), anhydrous potassium carbonate (2.40 g) and tetra-*n*-butylammonium bromide (1.33 g), and the mixture was heated under reflux for 90 min. After cooling, a large amount of water was added, and cream-color precipitates were separated from the solution by filtration. The crude product was purified by distilled water to give the target 1,2-bis(4-decyloxyphenyl) ethane-1,2-dione with a high yield (91.0%). ^{1}H-NMR ($CDCl_3$, 400 MHz): δ = 7.93 (d, 4H, ArH), 6.93 (d, 4H, ArH),

4.02 (t, 4H, －O－CH_2), 1.78–1.81 (m, 4H, －O－CH_2－CH_2), 1.27–1.45 (m, 28H, －CH_2), 0.86 (t, 6H, －CH_3). ^{13}C-NMR ($CDCl_3$, 101 MHz): δ = 189.03, 159.96, 127.83, 121.54, 110.08, 63.62, 27.35, 24.98, 24.76, 24.49, 21.35, 18.18. (See Supporting Information Fig. S2)

*5,8-Dibromo-2,3-bis(4-decyloxyphenyl)quinoxaline (**6**)*

Under a nitrogen atmosphere, a solution of 3,6-dibromo-1,2-phenylenediamine (1.33 g, 5 mmol) and 1,2-bis(4-decyloxyphenyl) ethane-1,2-dione (2.70 g, 5 mmol) in glacial acetic acid (65 mL) was heated under reflux for 12 h. Then the solution was cooled to 0 °C, added with 200 mL cooled alcohol, and filtered. The separated solid was washed with cooled EtOH for three times and dried in a vacuum oven to give 5,8-dibromo-2,3-bis(4-decyloxyphenyl) quinoxaline (2.63 g, 3.5 mmol) as a yellowish-white powder in the yield of 70.1%. ^{1}H-NMR ($CDCl_3$, 400 MHz): δ = 7.86 (s, 2H, ArH), 7.73 (d, 4H, ArH), 6.92 (d, 4H, ArH), 4.02 (q, 4H, －O－CH_2), 1.75–1.83 (m, 4H, －O－CH_2－CH_2), 1.14–1.48 (m, 28H, －CH_2), 0.88 (t, 6H, －CH_3). ^{13}C-NMR ($CDCl_3$, 101 MHz): δ = 161.32, 153.68, 139.41, 132.78, 131.81, 130.72, 123.59, 114.62, 68.51, 32.12, 29.63, 26.25, 22.82, 14.50. (See Supporting Information Fig. S3).

*Synthesis of **M1** and **M2***

In a dry 50 mL three necked round-bottomed flask, 5,8-dibromo-2,3-bis(4-decyloxyphenyl)quinoxaline (1.5 g, 2 mmol) and tributyl(3,4-dimethoxythiophen-2-yl) stannane or tributyl(2,3-dihydrothieno[3,4-b][1,4]dioxin-5-yl) stannane (8 mmol) were dissolved in anhydrous toluene (80 mL). The solution was intensely purged with nitrogen at room temperature for 30 min and bis(triphenylphosphine)palladium(II) chloride $Pd(PPh_3)_2Cl_2$ (0.14 g, 0.2 mmol) was added. Raise the temperature immediately until the solution was refluxed. The reaction mixture was stirred for 24 h under nitrogen atmosphere. Evaporation of the solvent under reduced pressure gave a crude mixture, which needed further separation by column chromatograph on silica gel (1:2, CH_2Cl_2/*n*-hexane). The purified product **M1** (2,3-bis(4-decyloxyphenyl)-5,8-bis(3,4-dimethoxylthiophen-2-yl)quinoxaline) is an orange solid (1.14 g, 64.9%). ^{1}H-NMR ($CDCl_3$, 400 MHz): δ = 8.54 (s, 2H, ArH), 7.70 (d, 4H, ArH), 6.88 (d, 4H, ArH), 6.40 (s, 2H), 3.98 (q, 4H, －O－CH_2), 3.91–3.87 (s, 12H, －O－CH_3), 1.77–1.81 (m, 4H, －O－CH_2－CH_2), 1.28–1.35 (m, 28H, －CH_2), 0.90 (t, 6H, －CH_3). ^{13}C-NMR ($CDCl_3$, 101 MHz): δ = 160.07, 150.93, 150.82, 145.77, 137.57, 132.57, 132.11,131.34, 129.63, 128.81, 121.06, 114.38, 99.18, 68.69, 68.26, 60.48, 57.44, 32.13, 29.82, 29.80, 29.65, 29.55, 29.51, 26.30, 22.91, 14.35. (See Supporting Information Fig. S4). MS ($C_{52}H_{66}N_2O_6S_2$) (*m*/*z*, EI+): calcd 879.22, found 879.29. The purified product **M2** (2,3-bis(4-decyloxyphenyl)-5,8-bis(2,3-dihydrothieno[3,4-b][1,4]dioxin-5-yl)quinoxaline) is an orange-red solid (1.20 g, 68.6%). ^{1}H-NMR ($CDCl_3$, 400 MHz): δ = 8.56 (s, 2H, ArH), 7.70 (d, 4H, ArH), 6.91 (d, 4H, ArH), 6.53 (s, 2H), 4.34 (dd, 8H, －O－CH_2－CH_2－O－), 4.00 (q, 4H, －O－CH_2), 1.77–1.82 (m, 4H, －O－CH_2－CH_2), 1.28–1.44 (m, 28H, －CH_2), 0.88 (t, 6H, －CH_3). ^{13}C-NMR ($CDCl_3$, 101 MHz): δ = 160.03, 150.54, 141.57, 140.41, 137.09, 132.57, 132.17, 131.34, 128.69, 127.81, 114.36, 113.76, 103.15, 68.26, 65.22, 64.57, 32.14, 29.82, 29.80, 29.66, 29.56, 29.52, 29.23, 26.31, 22.92, 14.35. (See Supporting Information Fig. S5). MS ($C_{52}H_{62}N_2O_6S_2$) (*m*/*z*, EI+): calcd 875.19, found 875.13.

RESULTS AND DISCUSSION

Synthesis

The reagent 4,7-dibromo-2,1,3-benzothiadiazole was reduced with an excess amount of $NaBH_4$ to give 3,6-dibromo-1,2-phenylenediamine (**2**) as a white solid. 1,2-Bis(4-methoxyphenyl) ethane-1,2-dione (**3**) was hydroxylated in a mixed solution of glacial acetic acid and hydrobromic acid, then the corresponding compound was alkylated with decylbromide *via* a common procedure[29]. The purified compound **2** and **5** was proceeded by condensation reaction in glacial acetic acid to afford 5,8-dibromo-2,3-bis(4-decyloxyphenyl) quinoxaline (**6**). Finally, the Stille coupling reaction of 5,8-dibromoquinoxalines with corresponding tributylstannane in the presence of $Pd(PPh_3)_2Cl_2$ as catalyst in anhydrous toluene solvent was carried out to give the title compound 2,3-bis(4-decyloxyphenyl)-5,8-bis(3,4-dimethoxylthiophen-2-yl)quinoxaline (**M1**) and 2,3-bis(4-decyloxyphenyl)-5,8-bis(2,3-dihydrothieno[3,4-b][1,4]dioxin-5-yl)quinoxaline (**M2**) in satisfactory yields (Scheme 1).

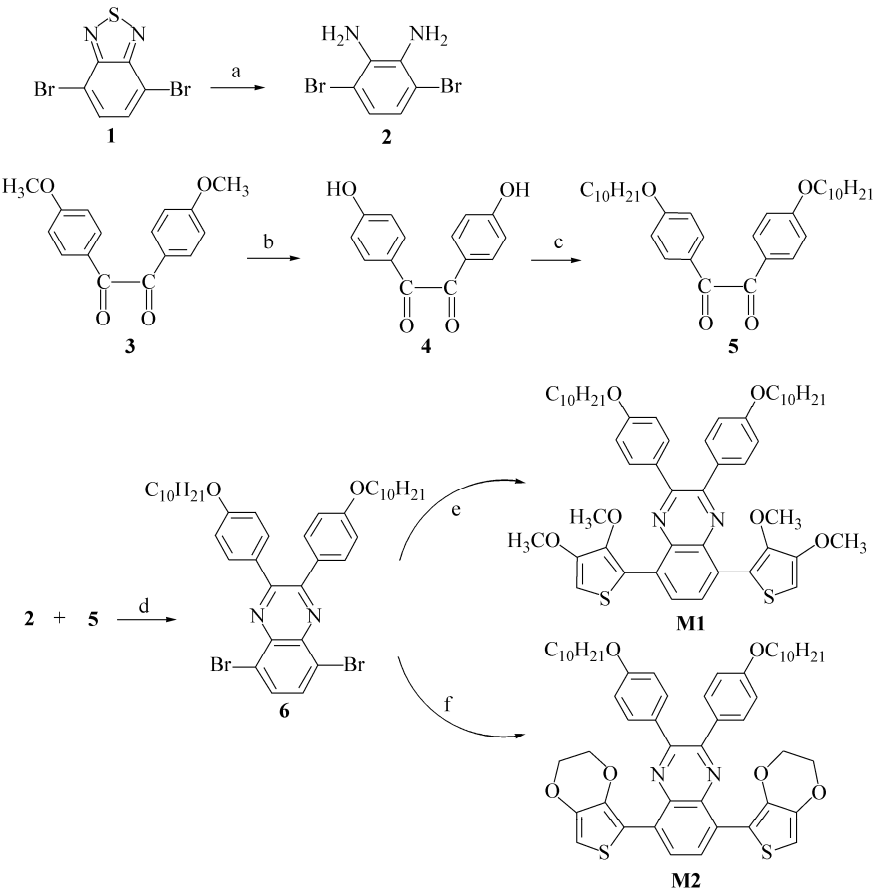

Scheme 1 Synthetic route to monomers, **M1** and **M2**

Both polymers were synthesized in a reaction medium containing 0.005 mol/L monomer and 0.2 mol/L tetrabutylammonium hexafluorophosphate ($TBAPF_6$) in a mixture solvent of acetonitrile (ACN) and dichloromethane (DCM) (3:1, by volume). The polymer films were synthesized on the working electrode (platinum wire or ITO/glass surface) by cyclic voltammetry (CV) or potentiostatic deposition, respectively.

Electrochemical Polymerization

Both **P1** and **P2** were polymerized on the platinum wire (the diameter is 0.5 mm) by cyclic voltammogram with repeated scanning between 0 V and 1.10 V and between −0.40 V and 1.10 V, respectively, at the same potential scan rate 100 $mV \cdot s^{-1}$. An explicit difference in redox behavior of polymers and the initial monomers can be seen from the CV depicted in Fig. 1. In cyclic voltammetry of the first lap, an irreversible monomer oxidation peak at 1.08 V for **M1**, 1.01 V for **M2** appeared, and the onset of oxidation potentials of **M1** and **M2** were calculated as 0.86 V and 0.82 V versus Ag wire pseudo reference electrode. Comparing initial oxidation potential of the monomers, **M2** can be oxidized relatively more easily than **M1** due to the existence of strong electron-donating ethylene-dioxy bridge on EDOT units compared to 3,4-dimethoxythiophen. As seen in Fig. 1, the current density of redox peak increased in the CVs, indicating the formation of the conductive polymers on the working electrode surface. With the elongation of the π-conjugated chain length, the initial oxidation potentials of **P1** and **P2** were further reduced to 0.35 V and 0.17 V, respectively. The voltammograms also suggested that both polymers showed two oxidation processes and a broad reduction process. **P2** showed two oxidation peaks at about 0.36 V and 1.04 V, which are lower than that of **P1** (0.72 V and 1.12 V). This result could also be attributed to the superior electron-donating ability of EDOT donor group which can give rise to a more efficient

D-A match and an extension of conjugate[30]. Through the above analysis, we can point out that higher donor capacity ethylene-dioxy groups on thiophenyl rings greatly affect the redox properties of monomers and polymers.

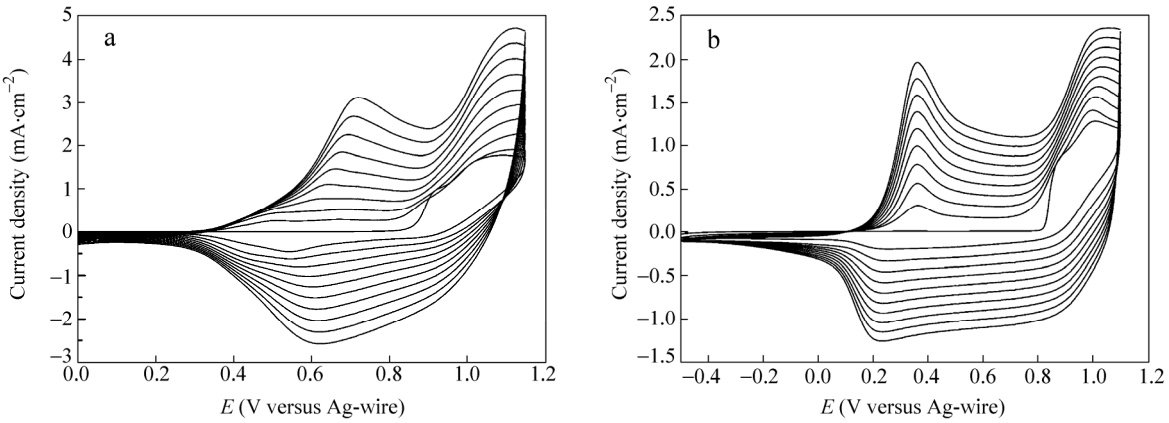

Fig. 1 Repeated potential-scan electropolymerization of **M1** (a) and **M2** (b) at 100 mV·s^{-1} in 0.2 mol·L^{-1} $TBAPF_6$/DCM/ACN on platinum wire electrode

Scan Rate Dependence and Stability

The direct relationship between the anodic and cathodic peak currents and scan rate of the polymer films which were prepared on Pt electrode with repeated scanning for three cycles were investigated by cyclic voltammetry at different scan rates. As shown in Fig. 2, both polymers exhibit reversible redox peaks at the positive potentials, and the maximum peak current density of the polymer films increases as the scan rate speeds up. A reversible redox couple of **P1** with an oxidation potential of 0.57 V and a reduction potential of 0.47 V was observed during the p-doping process. Similarly, the CV curves of **P2** exhibited an oxidation peak at about 0.30 V and a less obvious reduction peak at about 0.21 V. The scan rate dependence of the redox peak current density is illustrated in Fig. 2. Linear relationships were found between scan rates and peak currents which indicated that all polymer films were well adhered on the surface of working electrode and the charge transfer processes were not limited by diffusion effects[21].

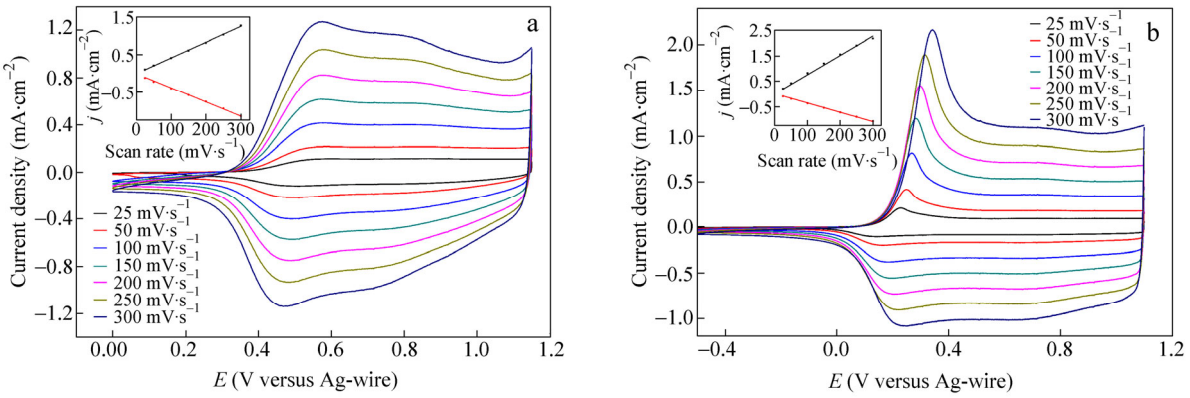

Fig. 2 Scan rate dependence of **P1** (a) and **P2** (b) films, electropolymerized on platinum electrode, at different scan rates between 25 and 300 mV·s^{-1} in the monomer-free 0.2 mol·L^{-1} $TBAPF_6$/ACN/DCM solution during p-doping process

In addition to the p-doping process of the polymer films, the n-doping electrochemical properties at the negative potentials were also investigated. As can be seen in Fig. 3, the initial reduction potentials of **P1** and **P2**

were −0.95 V and −0.94 V, respectively. Besides, both polymers were found to exhibit a quasi-reversible reduction and oxidation peak (E^{ox} = −1.35 V, E^{red} = −1.46 V for **P1**, and E^{ox} = −1.35 V, E^{red} = −1.45 V for **P2**) which indicates the n-style doping character of the films. By the contrast of the data it can be found that the oxidation-reduction potentials of the two polymers during n-doping process are so close to each other, which further confirms that N-doping behavior of the film mainly comes from the acceptor entity (decyloxyphenyl-quinoxaline) of the molecular chain. Furthermore, it is found that the redox peaks at the n-doped state were higher than those of the p-doping process for the polymers. This phenomenon was commonly occurred to the D-A type systems and is attributed to a combination of both n-doping and a redox transport mechanism[31, 32]. However, linear relationship between the scan rates and redox peak current of n-doping course was not as good as expected. This is most likely due to the degradation reaction of the films associated with water and air under a high negative potential. Besides, the spectral and color changes upon the reduction process were not detected.

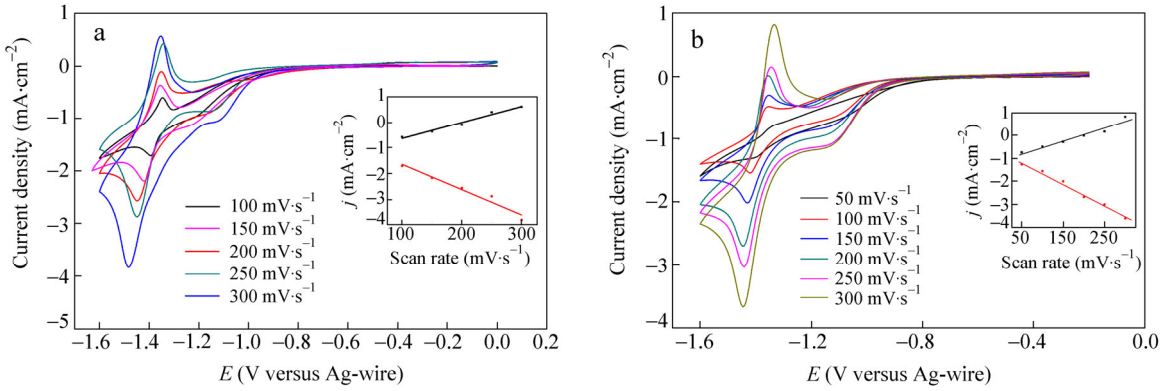

Fig. 3 (a) Scan rate dependence of **P1** film, electrochemically coated on platinum electrode, at different scan rates between 100 and 300 mV·s^{-1} in the monomer-free 0.2 mol·L^{-1} $TBAPF_6$/ACN/DCM solution during n-doping process. (b) Scan rate dependence of **P2** film, electrochemically coated on platinum electrode, at different scan rates between 50 and 300 mV·s^{-1} in the monomer-free 0.2 mol·L^{-1} $TBAPF_6$/ACN/DCM solution during n-doping process.

It is well known that the stability and robustness are critical for conducting polymers to be used in electrochromic applications, such as electronic devices and smart windows. In order to study the long-term switching stability, both polymers were deposited on platinum working electrode using CV method as described previously. The polymer films cycled between the neutral and oxidized states in a 0.1 mol·L^{-1} lithium perchlorate/propylene carbonate (PC) electrolyte/solvent couple at a potential scan rate of 200 mV·s^{-1} for 2500 times and 5000 times, respectively. As shown in Fig. 4(b), **P2** revealed outstanding redox stabilities with less than 1% decrease in total charge between the 1st and 2500th cycles and a decrease of less than 4% after sweeping 5000 cycles. Although the stability of **P1** was not as good as that of **P2**, 78% of the exchange charge still remained after 2500 cycles. It's important to note that the stable performance tests were carried out in ambient air, and the degradation reactions catalyzed with oxygen and trace water most probably caused the observed loss. If the covered electrode was assembled into electrochromic device, the stability upon switching between the neutral and oxidized states would be greatly improved. These results highlight the robustness and the good redox stability of both two hybrid polymer films, which make them good candidates for electrochromic applications.

Morphology

The surface morphologic structure is closely related to the electron transport and redox activity of conductive polymers. So the morphologies of the two polymer films, electrochemically coated on ITO/glass, were examined by SEM. The films can be readily prepared on ITO electrode at 1.1 V potentiostatically and dedoped before characterization. Pictures of the obtained hybrid polymer films are presented in Fig. 5. **P1** film exhibits a loose morphology with a heap of cerebelloid spheres pervading on the surface and the diameters of the spheres are

between 4 and 26 μm. **P2** film shows a comparatively compact structure with an ordered accumulation state of globules and interlinked porous channel among the clusters. These morphologies would prompt the doping anions to more efficiently soak into and come out of the films during the processes of doping and dedoping, in good agreement with the relatively good redox properties that were detected[33]. In addition, the thickness and unevenness of the above polymer films were measured by Step Profiler (Fig. 6). The average thickness of **P1** and **P2** were calculated as 1400 nm and 1000 nm, respectively. The extremely rough surface was disclosed in the images of the step profiler measurements, which is in keeping with the observed surface morphologies characteristic of scanning electron microscopy.

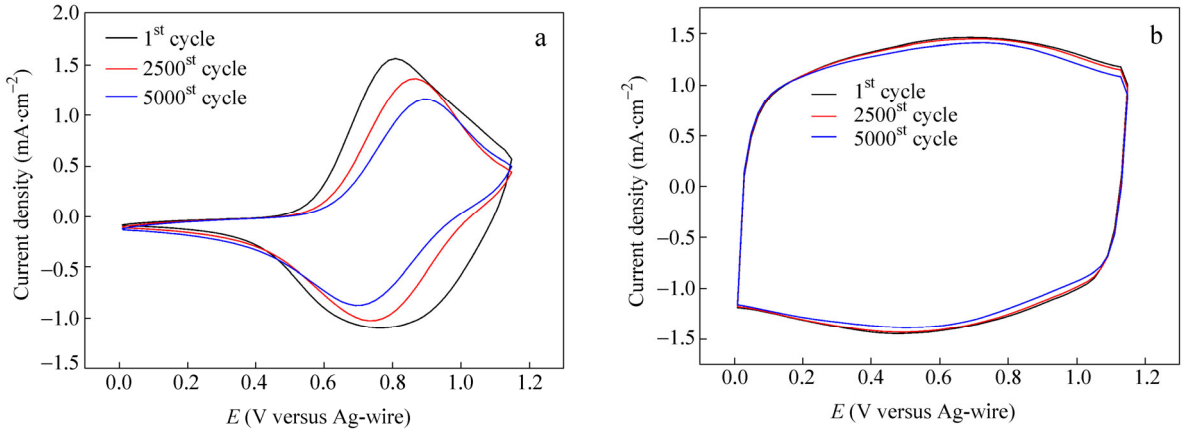

Fig. 4 Long-term cyclic voltammograms of the polymers **P1** (a) and **P2** (b) deposited on platinum wire in monomer free 0.1 mol·L^{-1} lithium perchlorate/propylene carbonate (PC) electrolyte/solvent couple

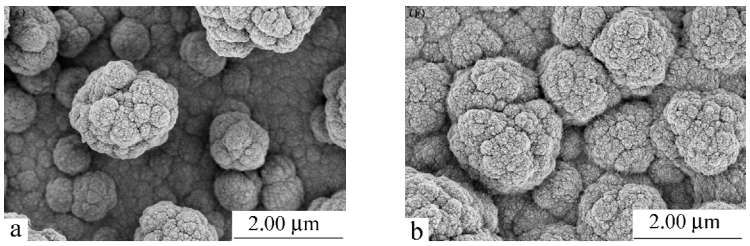

Fig. 5 SEM images of (a) **P1** and (b) **P2** deposited potentiostatically onto ITO/glass electrode

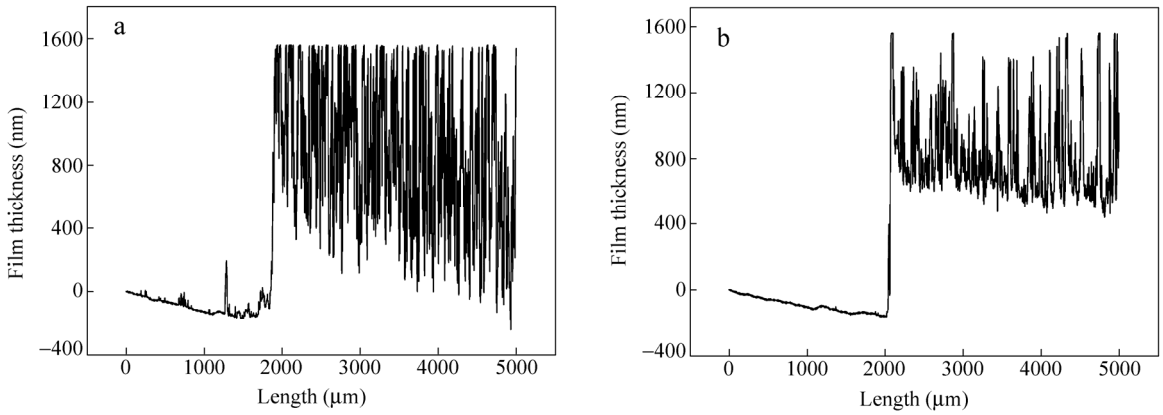

Fig. 6 Step profiler images of (a) **P1** and (b) **P2** deposited potentiostatically onto ITO/glass electrode

Optical Properties

The ultraviolet-visible spectra of the monomers in dichloromethane solution and their corresponding dedoped polymer in thin films are shown in Fig. 7 and the data are summarized in Table 1. Figure 7 reveals that both monomers exhibit two distinct characteristic absorption bands. The short wavelength absorption band is possibly due to the π-π^* electronic transition of thiophene-based segments, while the second band may be attributed to the donor-acceptor internal charge transfer (ICT) between the quinoxaline moiety, as the electron acceptor, and the thiophene-based units, as the electron donor[34]. Two obvious absorption peaks were observed at 311 nm and 401 nm for **M1**, and 321 nm and 462 nm for **M2**. According to the UV-Vis spectra data of the monomers, the optical band-gap values of the monomers were found to be 2.42 eV and 2.31 eV, respectively, as calculated from the lowest energy absorption edges (λ_{onset} = 513 nm for **M1**, 537 nm for **M2**). By contrast with monomer **M1**, bathochromic shift in the maximum absorption band and reduction in band gap of **M2** were due to the introduction of the electron donating effect of the ethylene-dioxy group on thiophenyl ring. The ethylene-dioxybridge caused less steric hindrance than dialkoxy side chains, thus resulted in a more efficient overlapping between the π-orbital of oxygen atom and the conjugated system. This effect is much more obvious in the long chain polymers, where a 146 nm red shift was observed for **P2** film. Additionally, an obvious red shift in the maximum absorption peak for polymers compared to their respective monomers owing to the increased conjugation length was observed, and the corresponding optical and electrochemical data are listed in Table 1.

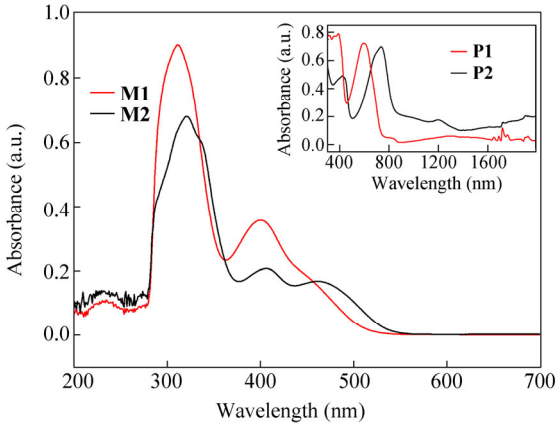

Fig. 7 UV-Vis absorbance spectra of **M1** and **M2** in DCM (Inset: absorption spectra of the corresponding polymers deposited on ITO at the neutral state.)

Table 1. The onset oxidation potential ($E_{ox,onset}$), the onset reduction potential ($E_{red,onset}$), absorption onset wavelength (λ_{onset}), HOMO and LUMO energy levels, electrochemical band gap ($E_{g,ec}$) and optical band gap ($E_{g,op}$) of the monomers and their corresponding polymers

Sample	$E_{ox,onset}$ versus Ag (V)	$E_{red,onset}$ versus Ag (V)	λ_{onset} (nm)	$E_{g,op}$ [a] (eV)	E_{HOMO} [b] (eV)	E_{LUMO} [c] (eV)	$E_{g,ec}$ [d] (eV)
M1	0.86	–	513	2.42	–5.26	–	–
M2	0.82	–	537	2.31	–5.22	–	–
P1	0.35	–0.95	750	1.65	–4.75	–3.45	1.30
P2	0.17	–0.94	854	1.45	–4.57	–3.46	1.11

[a] Calculated from the low energy absorption edges (λ_{onset}), $E_{g,op}$= 1241/λ_{onset};
[b] E_{HOMO} = –($E_{ox,onset}$ + 4.4) ($E_{ox,onset}$ versus Ag);
[c] E_{LUMO} = –e($E_{red,onset}$+ 4.4) ($E_{red,onset}$ versus Ag);
[d] $E_{g,ec}$ = E_{LUMO}–E_{HOMO}.

In addition, to better understand the geometric structures and electrical band gaps of the monomers, the density functional theory (DFT) was carried out for the monomers of **M1** and **M2** by employing the Gaussian 03 program. The HOMO (highest occupied molecular orbital) and LUMO (lowest unoccupied molecular orbital)

profiles are illustrated in Fig. 8. It is found that the ground-state charge distributions of the HOMO and LUMO showed significant difference on the distribution pattern. The LUMO wave functions are mainly localized on the phenylquinoxaline acceptor moieties, while the HOMO wave functions are delocalized along the thiophene donors and the adjacent aromatic rings. Through simulation and calculation, the band gaps are calculated to be 2.96 eV and 2.84 eV for **M1** and **M2** respectively. The band gap value of **M2** calculated by density functional theory is lower than that of **M1**, which is in good agreement with optical experiment results. However, the theoretical simulation values were found to be higher than the test data, which could be caused by various influence factors, such as solvent effects and variation of physical form from the solid states to the gaseous states[35].

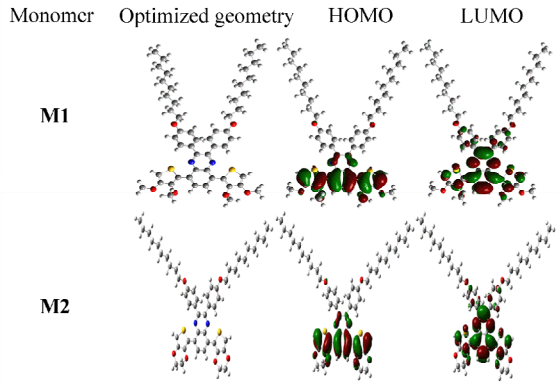

Fig. 8 The optimized geometries and the molecular orbital of the HOMOs and LUMOs for **M1** and **M2**

Spectroelectrochemistry

Spectroelectrochemical measurements were performed during stepwise oxidation process using a UV-Vis-NIR spectrophotometer coupled with electrochemical workstation to better understand the optical changes upon doping of the quinoxaline based cross-linked polymers. Two polymer films were potentiostatically deposited on ITO/glass electrode at 1.10 V with the polymerization charge about 2.0×10^{-2} C, respectively. The attached films on ITO/glass were washed three times using ACN/DCM mixture solution to remove the $TBAPF_6$ electrolyte, the residual monomers and some of the oligomers. Then the *in situ* UV-Vis-NIR spectra of the films at various applied potentials from 0 V to 1.1 V for **P1** and −0.4 V to 1.1 V for **P2** were investigated in monomer-free 0.2 mol/L $TBAPF_6$/ACN/DCM solution.

As shown in Fig. 9, both polymers exhibit two absorption peaks at the neutral state assigned to the transitions from the thiophene-based valence band to its antibonding band (high-energy π-π^* transition) and weak intramolecular charge transfer band, which is the nature of donor-acceptor conjugate system. Two characteristic absorption bands of **P1** are located at 387 and 595 nm, giving rise to a blue color in the neutral state. However, as for **P2** thin film, favorable matches between the electron-accepting quinoxaline group and the electron-donating EDOT units increased the double-bond character and strengthened the conjugation effect among the polymer chain, thus allowing absorption of low-energy photons and resulting in the red shift of the absorption wavelengths. As a result, **P2** showed two red shifted maximum absorption wavelengths at both 423 and 742 nm, which is necessary for a saturated green color to be obtained in the neutral state.

As shown in Fig. 9, upon progressive oxidation of the polymers, new absorption band appeared in NIR while the strong visible light absorption spectrum was gradually depleting. The newly formed lower-energy electronic absorption peaks are believed to associate with the formation of charge carriers such as polarons and bipolarons. For **P1**, polaronic absorption band at 832 nm was observed at low doping levels. While at the fully oxidized state, all the absorption peaks mentioned above vanished with the only left broad absorption band extending into the IR region, which indicated to the polymer film that the formation of bipolaronic states had occured. **P2** also showed the similar tendencies in the absorption spectra change. And, both polymers revealed

highly transmissive light grey color in their fully oxidized states due to the depletion of the absorption across the visible region. Additionally, for polymers **P1** and **P2**, the spectra also revealed two well-define disosbestic points at around 700 nm and 805 nm, respectively, which indicates that two distinct forms (the neutral form and radical cation) of the polymers can be well interconverted.

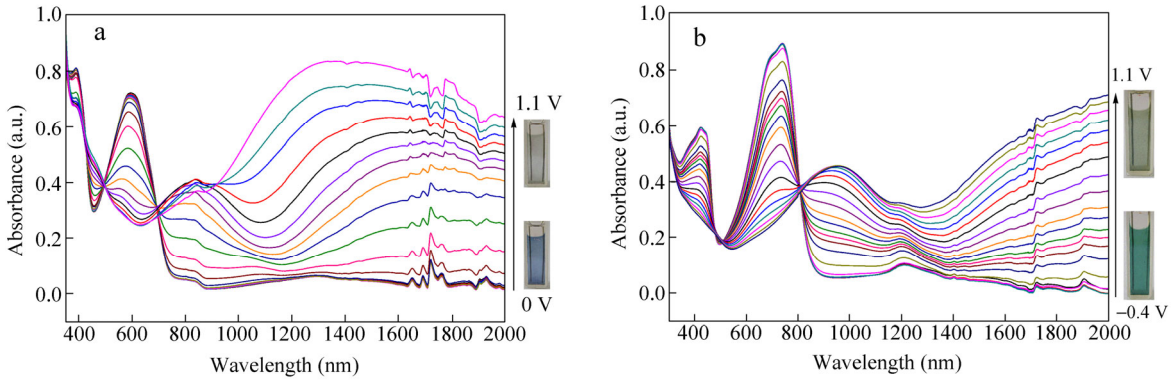

Fig. 9 (a) Spectroelectronic absorption spectra and the color changes of **P1** deposited onto ITO/glass surface with the applied potential of 0–1.1 V in the monomer-free 0.2 mol·L^{-1} TBAPF6/ACN/DCM on p-doping; (b) Spectroelectronic absorption spectra and the color changes of **P2** deposited onto ITO/glass surface with the applied potential of –0.4–1.1 V in the monomer-free 0.2 mol·L^{-1} TBAPF$_6$/ACN/DCM on p-doping

Electrochromicswitching Studies

The electrochromic switching ability of polymer film was investigated by double potential step chronoamperometry technique coupled with optical spectroscopy during repeated potential stepping between their neutral and fully oxidized states with a regular time interval of 4 s at given wavelengths both in the visible and NIR regions. These electrochromic switching behaviors of the two conducting polymer films (electropolymerized-coated on ITO/glass) were performed in a monomer-free ACN/DCM (1: 1, by volume) solution containing 0.2 mol·L^{-1} TBAPF$_6$ as a supporting electrolyte.

One of the crucial factors, the optical contrast of the polymer films which can be defined as the percent transmittance change between the redox states at some specific wavelengths is depicted in Fig. 10. The optical contrasts of the **P1** film by switching between 0 V (the neutral) and 1.1 V (the oxidized state) were found to be 42%, 30% and 69% at 595, 839, and 1500 nm, respectively. Response time, another important characteristic of the electrochromic materials, is the necessary time for 95% of the full optical switch. Through analyzing, the **P1** film can switch very rapidly between the neutral and oxidized state with the response times less than 1 s (which were calculated to be 0.8 s at 595 nm and 839 nm, and 0.4 s at 1500 nm) both in the visible and NIR regions. The optical contrasts and the response times from reduced to oxidized state of **P2** film at different wavelengths were also investigated and summarized in Table 2. Furthermore, as seen from Fig. 10, slight losses in the percent transmittance contrast value after regular switching during 300 s, indicating the robustness and the stability of the system. Through the above analysis, polymers synthesized in present work showed the ability to switch rapidly, to exhibit striking transmittance change and high stability upon repeated cycles, which suggested the promising potential applications in electrochromic devices and optical displays.

Table 2. The optical contrasts (ΔT%), response times and coloration effciencies (CE) of **P1** and **P2** at different wavelengths

Compounds	λ (nm)	Optical contrast (ΔT%)	Response time (s)	CE (cm^2·C^{-1})
P1	595	42	0.8	251
	839	30	0.8	204
	1500	69	0.4	339
P2	740	32	0.3	135
	2000	71	0.4	370

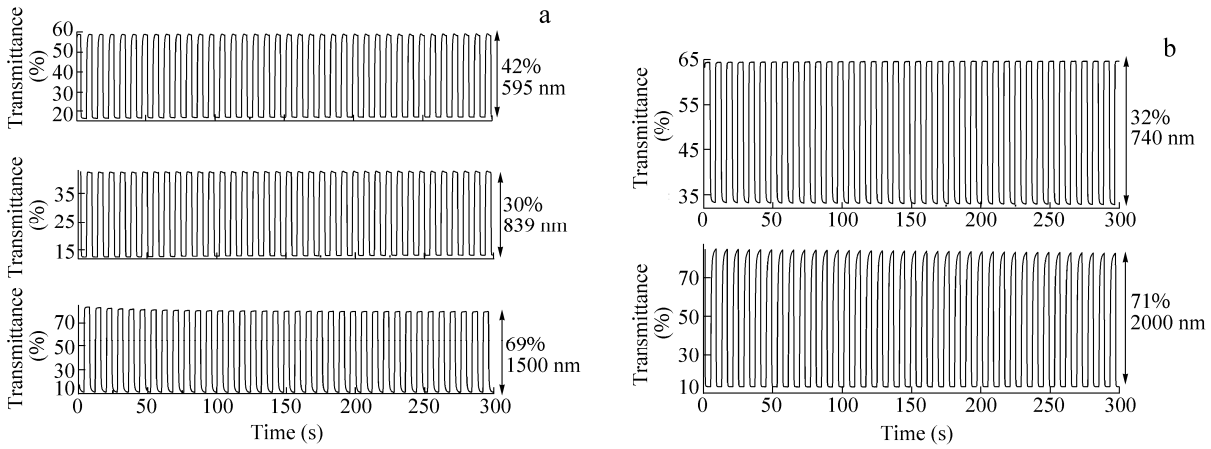

Fig. 10 (a) Electrochromic switching, percent transmittance change monitored at 595, 839 and 1500 nm for **P1** between 0 and 1.1 V; (b) Electrochromic switching, percent transmittance change monitored at 740 and 2000 nm for **P2** between –0.4 V and 1.1 V

The coloration efficiency (CE) is also another important index of evaluating the electrochemical properties of the electrochromic materials as it describes the change in optical density (ΔOD) for the charge consumed per unit electrode area (ΔQ)[36] at a specific dominant wavelength according to equations[37]: $\eta = \Delta OD/\Delta Q$ and $\Delta OD = \lg(T_b/T_c)$, where T_b and T_c are the transmittances before and after doping, respectively, and ΔQ is the amount of injected/ejected charge per unit sample area. According to the equations mentioned above, CE of **P1** film was calculated as 251 $cm^2 \cdot C^{-1}$ (at 595 nm), 204 $cm^2 \cdot C^{-1}$ (at 839 nm) and 339 $cm^2 \cdot C^{-1}$ (at 1500 nm), respectively, by monitoring the charge and change in transmittance. And for **P2** film, the CE data were measured as 135 $cm^2 \cdot C^{-1}$ at 740 nm and 370 $cm^2 \cdot C^{-1}$ at 2000 nm. It's worth noting that both high optical contrasts and considerable coloration efficiencies in the NIR region for the two polymers make these electrochromic materials good candidates to be used in NIR applications[38].

CONCLUSIONS

In summary, two novel π-conjugated polymers containing electron deficient 2,3-bis(4-decyloxyphenyl)-quinoxaline acceptor and different alkoxythiophene donors were synthesized. Their corresponding electroactive polymers were electrochemically deposited on platinum-wire electrode or ITO/glass electrode surface to investigate the electrochemical and spectroelectrochemical properties of resultant hybrid conducting polymers, respectively. Both polymer films exhibited well-defined reversible redox behavior, good long-term switching stability and reasonable n-doping process. By contrast with the experiment data of 3,4-dimethoxylthiophen substituted quinoxalines, the strong electron-donating EDOT results in the decrease of oxidation potentials and electronic band-gap of the monomer and polymer, which can be attributed to the steric hindrance effect. Besides, the density functional theory (DFT) was employed to better understand the geometric structures and electronic properties of the monomers. Except for electrochemical performance, altering the electron-donating substitutes also has an enormous effect on the photoelectric properties of the resulting polymers. **P1** was blue in neutral state with two maximum absorption peaks at 387 and 595 nm in the visible region, while **P2** thin film turned to blue-green in accordance with the red shift of the absorption wavelengths due to the favorable matches between the quinoxaline acceptor and the EDOT donor units. As expected, both polymers in the completely oxidized state are almost colorless and transparent with the only left strong absorption band extending into the NIR region which is of high interest in electrochromic field. In general, the combination of promising large optical contrasts, high coloration efficiencies, and especially considerably fast response times proved the potential use for these hybrid polymers in electrochromic device applications.

REFERENCES

1 Garcia, A., Bakus, R.C., Zalar, P., Hoven, C.V.J., Brzezinski, Z. and Nguyen, T.Q., J. Am. Chem. Soc., 2011, 133: 2492
2 Beaujuge, P.M., Pisula, W., Tsao, H.N., Ellinger, S., Müllen, K. and Reynolds, J.R., J. Am. Chem. Soc., 2009, 131: 7514
3 Renuga, D., Udhayakumari, D., Suganya, S. and Velmathi, S., Tetrahedron Lett., 2012, 53: 5068
4 McQuade, D.T., Pullen, A.E. and Swager, T.M., Chem. Rev., 2000, 100: 2537
5 Nicho, M.E., Hailin, H., López-Mata, C. and Escalante, J., Sol. Energ. Mater. Sol. C., 2004, 82: 105
6 Sefer, E., Koyuncu, F.B., Oguzhan, E. and Koyuncu, S., J. Polym. Sci., Part A: Polym. Chem., 2010, 48: 4419
7 Zoombelt, A.P., Fonrodona, M., Turbiez, M.G.R., Wienk, M.M. and Janssen, R.A.J., J. Mater. Chem., 2009, 19: 5336
8 Kim, J., Cho, N., Ko, H.M., Kim, C., Lee, J.K. and Ko, J., Sol. Energ. Mater. Sol. C., 2012, 102: 159
9 Ramya, R., Sivasubramanian, R. and Sangaranarayanan, M.V., Electrochim. Acta, 2013, 101: 109
10 Walker, W., Veldman, B., Chiechi, R., Patil, S., Bendikov, M. and Wudl, F., Macromolecules., 2008, 41: 7278
11 Persson, N.K., Sun, M., Kjellberg, P., Pullerits, T. and Inganäs, O., J. Chem. Phys., 2005, 123: 204718
12 Sakthivel, P., Song, H.S., Chakravarthi, N., Lee, J.W., Gal, Y.S., Hwang, S. and Jin, S.H., Polymer, 2013, 54: 4883
13 Zoombelt, A.P., Leenen, M.A.M., Fonrodona, M., Nicolas, Y., Wienk, M.M. and Janssen, R.A.J., Polymer, 2009, 50: 4564
14 Cihaner, A. and Algı, F., Adv. Funct. Mater., 2008, 18: 3583
15 Xu, Z., Wang, M., Zhao, J.S., Cui, C.S., Fan, W.Y. and Liu, J.F., Electrochim. Acta, 2014, 125: 241
16 Xu, Z., Wang, M., Fan, W.Y., Zhao, J.S. and Wang, H.S., Electrochim. Acta, 2015, 160: 271
17 Hou, Y.F., Xu, G.Q., Zhao, J.S., Kong, Y. and Yang, C., Acta. Chim. Sinica, 2014, 72: 1238
18 Groenendaal, L., Zotti, G., Aubert, P.H., Waybright, S.M. and Reynolds, J.R., Adv. Mater., 2003, 15: 855
19 Kvarnstrom, C., Neugebauer, H., Blomquist, S., Ahonen, H.J., Kankare, J. and Ivaska, A., Electrochim. Acta, 1999, 44: 2739
20 Gunbas, G.E., Durmus, A. and Toppare, L., Adv. Funct. Mater., 2008, 18: 2026
21 Sonmez, G., Schwendeman, I., Schottland, P., Zong, K. and Reynolds, J.R., Macromolecules, 2003, 36: 639
22 Heywang, G. and Jonas, F., Adv. Mater., 1992, 4: 116
23 Hanna, R. and Leclerc, M., Chem. Mater., 1996, 8: 1512
24 Sonmez, G., Sonmez, H.B., Shen, C.K.F., Jost, R.W., Rubin, Y. and Wudl, F., Macromolecules, 2005, 38: 669
25 Li, M., Sheynin, Y., Patra, A. and Bendikov, M., Chem. Mater., 2009, 21: 2482
26 Tsubata, Y., Suzuki, T., Miyashi, T. and Yamashita, Y., J. Org. Chem., 1992, 57: 6749
27 Zhao, H., Wei, Y.Y., Zhao, J.S. and Wang, M., Electrochim. Acta, 2014, 146: 231
28 Zhu, S.S. and Swager, T.M., J. Am. Chem. Soc., 1997, 119: 12568
29 Mohr, B., Enkelmann, V. and Wegner, G., J. Org. Chem., 1994, 59: 635
30 Berlin, A., Zotti, G., Zecchin, S., Schiavon, G., Vercelli, B. and Zanelli, A., Chem. Mater., 2004, 16: 3667
31 DuBois, C.J., Abboud, K.A. and Reynolds, J.R., J. Phys. Chem. B., 2004, 108: 8550
32 DuBois, C.J. and Reynolds, J.R., Adv. Mater., 2002, 14: 1844
33 Ozkut, M.I., Atak, S., Onal, A.M. and Cihaner, A., J. Mater. Chem., 2011, 21: 5268
34 Jespersen, K.G., Beenken, W.J.D., Zaushitsyn, Y., Yartsev, A., Andersson, M.R., Pullerits, T. and Sundstrom, V., J. Chem. Phys., 2004, 121: 12613
35 Zhao, H., Tang, D.D., Zhao, J.S., Wang, M. and Dou, J.M., RSC Adv., 2014, 4: 61537
36 Deepa, M., Awadhia, A. and Bhandari, S., Phys. Chem. Chem. Phys., 2009, 11: 5674
37 Bechinger, C., Burdis, M.S. and Zhang, J.G., Solid State Commun., 1997, 101: 753
38 McDonagh, A.M., Bayly, S.R., Riley, D.J., Ward, M.D., McCleverty, J.A., Cowin, M.A., Morgan, C.N., Varrazza, R., Penty, R.V. and White, I.H., Chem. Mater., 2000, 12: 2523